Molecular Imaging and Biology (2023) 25:1020–1033
https://doi.org/10.1007/s11307-023-01856-z

REVIEW ARTICLE

Magnetic Particle Imaging-Guided Hyperthermia for Precise Treatment of Cancer: Review, Challenges, and Prospects

Siao Lei[1,2,3] · Jie He[1,2,3] · Pengli Gao[1,2,3] · Yueqi Wang[3] · Hui Hui[3] · Yu An[1,2,3] · Jie Tian[1,2,3,4]

Received: 10 April 2023 / Revised: 2 September 2023 / Accepted: 5 September 2023 / Published online: 3 October 2023

Abstract

Magnetic particle imaging (MPI) is a novel quantitative imaging technique using the nonlinear magnetization behavior of magnetic nanoparticles (MNPs) to determine their local concentration. Magnetic fluid hyperthermia (MFH) is a promising non-invasive therapy using the heating effects of MNPs. MPI-MFH is expected to enable real-time MPI guidance, localized MFH, and non-invasive temperature monitoring, which shows great potential for precise treatment of cancer. In this review, we introduce the fundamentals of MPI and MFH and their applications in the treatment of cancer. Also, we discuss the challenges and prospects of MPI-MFH.

Key words Magnetic particle imaging · Magnetic fluid hyperthermia · Cancer · Precise treatment

Introduction

Cancer diagnostics is a method that combines diagnosis and therapeutics of cancer diseases, which involves nanomaterial preparation, bioprobe targeting, molecular imaging, and minimally invasive treatment [1]. It is increasingly clear that ultrasensitive and quantitative measurement of theranostic biomarkers and efficient identification, visualization of cancer at its earliest stage with high resolution and in a quantitative manner, molecular targeting, and localized treatment will all be critical for precision treatment of cancer [2].

The traditional treatment methods for cancer include surgery, radiation therapy, and chemotherapy. The primary treatment method for cancer is surgery, but it is generally suitable only in early stages of cancer [3]. Most patients are not suitable for surgical treatment in the late stages, such as breast cancer [4] and pancreatic cancer [5]. Radiation therapy mainly uses high-energy radiation, such as X-rays and gamma-rays, to create energy directly to kill cancer cells or inhibit their growth [6]. The main limitations of traditional radiation therapy lie in the radiation that also produces radioactive doses in normal tissues, leading to persistent patient harm, and may have long-term side effects [7]. Proton therapy, a more accurate and effective radiation therapy, uses high-energy proton beams to directly kill cancer cells [8]. This method reduces the side effects of radiation therapy significantly by killing only the cancer cells with little harm to healthy cells [9]. However, the price is high because it requires high-quality treatment facilities [10]. Chemotherapy works by using cytotoxic drugs to inhibit cell proliferation [11]. Most chemotherapy drugs must be close to their maximum tolerated dose to function, which means chemotherapy is toxic to the whole body [12]. This leads to various side effects and gradually decreases the patient's immune function [13]. Magnetic fluid hyperthermia (MFH), as a new therapeutic technology, uses high-frequency excitation to generate electromagnetic waves produced by the magnetic field, based on relaxation loss or hysteresis loss to heat the tumors to about 43 °C, to kill cancer cells through high

Siao Lei and Jie He contributed equally to this work.

✉ Yu An
yuan1989@buaa.edu.cn

✉ Jie Tian
tian@ieee.org

1 School of Engineering Medicine & School of Biological Science and Medical Engineering, Beihang University, Beijing 100191, China

2 Key Laboratory of Big Data-Based Precision Medicine (Beihang University), Ministry of Industry and Information Technology of the People's Republic of China, Beijing 100191, People's Republic of China

3 CAS Key Laboratory of Molecular Imaging, Institute of Automation, Beijing 100190, China

4 Zhuhai Precision Medical Center, Zhuhai People's Hospital, Affiliated With Jinan University, Zhuhai 519000, China

temperature. This technology has the advantages of non-invasive, radiation-free, no disease-forming, and low treatment costs compared to the above treatment methods. It has little toxicity to the healthy tissues [14].

Hyperthermia has been widely studied in recent years. This process does not directly kill the cells but leads to the initiation of a series of pro-apoptotic and apoptotic signaling cascades [15], which finally induces cell death. Heat can slow or stop tumor growth by damaging or killing cancer cells by damaging proteins, structures, and blood vessels within the tumor [14]. The heat can induce the increase in some proteins in the lesion site, such as γ-H2AX, which can cause DNA damage or apoptosis, making cancer cells more vulnerable to radiation therapy and chemotherapy in subsequent treatments [16]. Meanwhile, the heat also modifies the blood circulation to deliver oxygen to the tumor tissue, making the tumor cells more sensitive to radiation therapy and chemotherapy [17]. Cellular responses to heat stress can also promote the expression of heat shock proteins, which can induce an organism's immunity to tumor cells [18]. Therefore, hyperthermia is increasingly used in combination with radiotherapy [19] and chemotherapy [20] to treat solid tumors. In the conducted clinical studies by Deger [21] et al., the combination of heat therapy and radiotherapy was applied to prostate cancer. After treatment, prostate-specific antigen (PSA) was significantly lowered. Brero et al. [22] effectively demonstrated the radiosensitization of hyperthermia to pancreatic cancer cells by combining proton therapy and MFH, and the proton therapy they used was synergistically cooperative with MFH. Singh et al. [23] compared the individual effects of heat therapy and chemotherapy with the combination therapy in prostate cancer and found that the combination therapy had significant efficiency in suppressing tumor growth.

Researchers have proposed many different hyperthermia methods. A comparison of their classifications and applications is summarized in Table 1.

A treatment method needs to be guided by the appropriate imaging mode to achieve the purpose of accurate treatment. Magnetic particle imaging (MPI) is a novel quantitative imaging technique with its advantages of high sensitivity and resolution, which uses the nonlinear magnetization behavior of magnetic nanoparticles (MNPs) [41]. In this review, we discuss MPI-guided MFH (MPI-MFH) and its application in cancer.

In the following, we briefly introduced MPI and MFH in this section, including their basic principles, features, and devices. Then, we showed some typical applications of image-guided MFH in cancer therapy, illustrating the potential of MPI-guided MFH in cancer precision therapy. The MNPs, targeted modified MNPs, and their application in MPI and MFH are then presented. Lastly, we discuss the current challenges of MPI-MFH. In addition, we look ahead

Table 1 A comparison of different hyperthermia methods

Type	Motivations	Limitations	Applications
Radiofrequency	High heat conversion efficiency and minimally invasive	Easy to cause damage to surrounding healthy tissues	Liver cancer [24], bladder cancer [25], and rectal cancer [26]
Microwave	Generating heat fast and penetrating deep	Inaccurate targeting, low selectivity, and causing damage to surrounding healthy tissues	Prostatic hyperplasia [27] and melanoma [28]
Ultrasonic	Minimally invasive and simple to implement	Does not easily penetrate certain tissues, such as the skull [9]	Pancreatic cancer [29], uterine fibroids [30], and thyroid nodules [31]
Photothermal therapy	High specificity and little side effect on normal tissues	Uneven distribution of heat and causing damage to healthy tissues around tumors [32, 33]	Ovarian cancer [34] and sentinel lymph node [32]
Photodynamic therapy	Non-invasive, no long-term adverse reactions, and quick recovery	Does not deep enough and only suitable for the treatment of superficial lesions [35]	Lung cancer [36]
Magnetic fluid hyperthermia	No ionizing radiation, no depth limitation, non-invasive, and reducing damage to healthy tissue	Low magneto-thermal conversion efficiency and off-target accumulation of heat for healthy organs	Breast cancer [37], ovarian cancer [38], prostate cancer [39], and glioma [40]

to the future of MPI-MFH and other applications in precise treatment of cancer.

Introduction of MPI and MFH

MPI

MPI has been extensively used in studies including hemodynamic evaluation [42], cardiac imaging [43], cell tracing [44, 45], cancer imaging [46], perfusion imaging [47], and prediction of the MFH effect [40]. The MPI device simply consists of the selection coils or permanent magnets that generate a field-free region (FFR), the drive coils that excite the nonlinear magnetization behavior of MNPs, and the receiver coils that induce changes of the magnetization of MNPs (Fig. 1) [48]. The magnetization dynamics of MNPs are very complex and can be simplified to the Langevin theory description under the assumption that MNPs are in a constant thermal equilibrium [49].

MPI signals also hold promise for temperature imaging. Relaxation processes are temperature dependent, so it is expected to estimate the sample temperature from the magnetization response signals of MNP samples [50].

Since the first MPI scanner for small animals was proposed in 2005 [41], the development of MPI devices has made great progress, as reported in [51]. We reviewed the development of MPI devices, as shown in Fig. 2. Currently, two commercial devices have been developed, one from Bruker and the other from Magnetic Insight. In 2014, traveling wave magnetic particle imaging (TWMPI) was proposed to generate a dynamic gradient field system that can cover a larger field of view, providing a new direction for large bore device development [52]. For the development of a large bore size of MPI, Graeser et al. proposed a human-sized MPI system suitable for the detection of human heads [53]. Over the past 2 years, MPI devices have made progress in increasing the bore size and individual functions [54].

As a new imaging method, MPI has many advantages:

- MPI has good penetration and signal-to-noise ratio;
- The MPI signal has no radiation and does not harm the human body [51];
- The MPI signal will not undergo radioactive decay over time [55];
- MPI has real-time imaging capabilities to provide immediate feedback [56, 57];
- MPI is expected to realize the detection of multiple parameters, such as temperature and viscosity [58, 59].

MFH

Under the induction of an AMF, MNPs generate heat through relaxation loss or hysteresis loss [60]. According to Rosensweig's theory [61], the average volume energy dissipation rate of magnetic particles per period under the action of alternating magnetic fields is defined as follows:

$$P = f\Delta U = -f\mu_0 \oint MdH$$

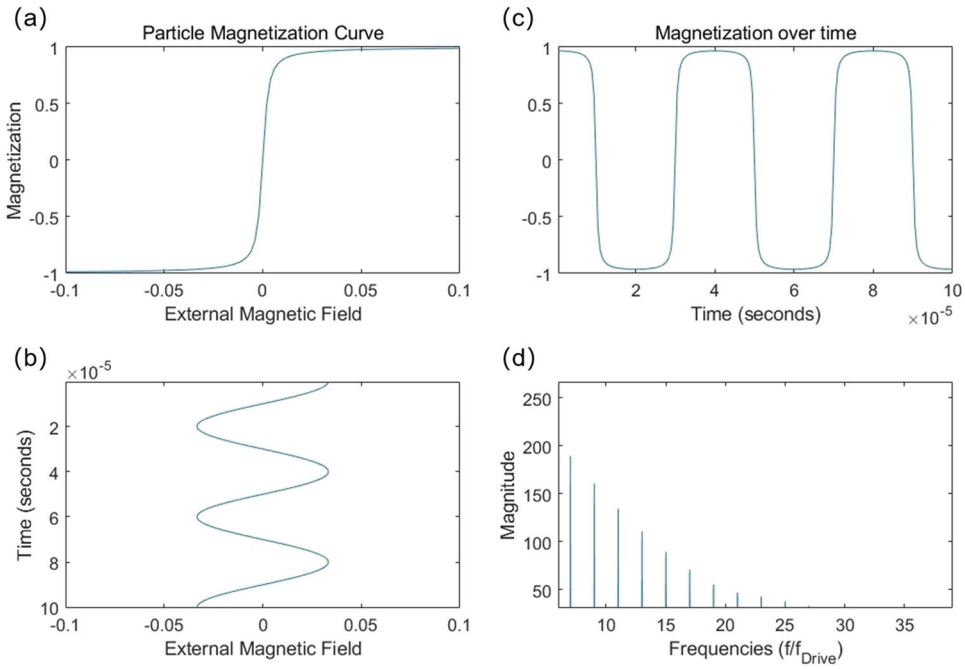

Fig. 1 Illustration of the principle of MPI. **a** M-H curve under Langevin's model. **b** Exciting magnetic field. **c** Time-dependent magnetization. **d** Fourier-transformed signal

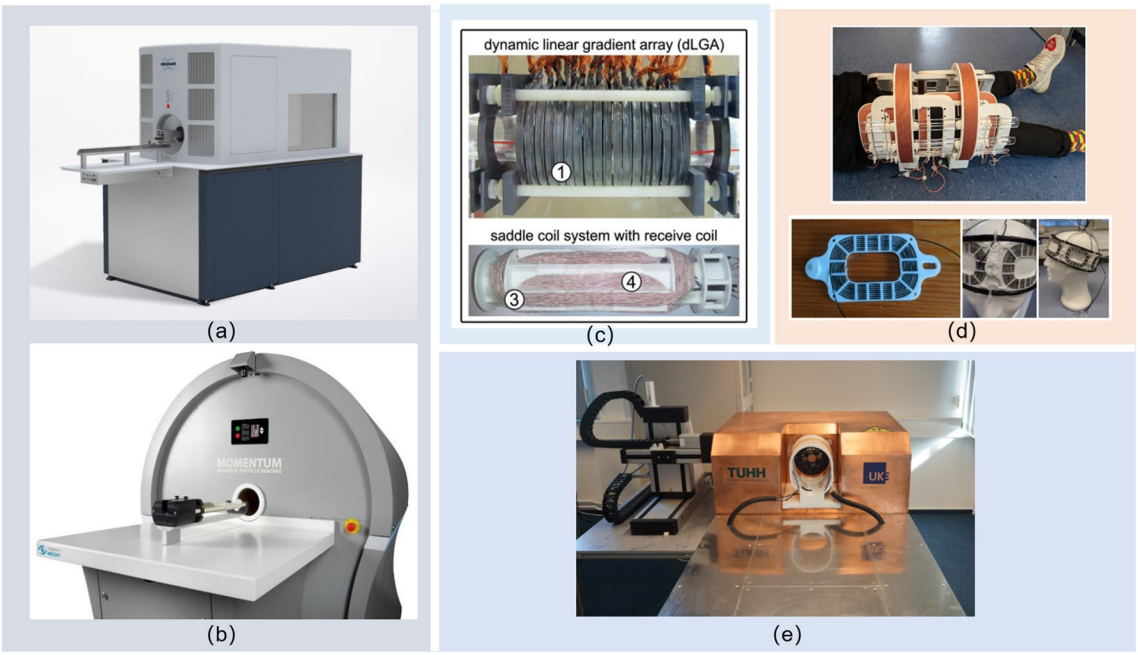

Fig. 2 The main devices of MPI. **a** The device from Bruker. **b** The device from Magnetic Insight. **c** TWMPI scanner. **d** Human-sized interventional MPI scanner and human-sized wearable brain scanner. **e** Human-sized MPI for brain applications. **a** From http://www.bruker.com; **b** from http://www.magneticinsight.com; **c** from [52], **d** from [54]; **e** from [53]

where f and H are the frequency and amplitude of the applied magnetic field, respectively, M is the particle magnetic moment, and μ_0 is the vacuum permeability.

The heating capacity of MNPs is defined as the specific absorption rate (SAR), expressed as the heating power (P) produced per unit mass of MNPs(m_{MNP}):

$$SAR = \frac{P}{m_{MNP}} = C\left(\frac{\Delta T}{\Delta t}\right)\left(\frac{1}{m}\right)$$

where C is the sample-specific heat capacity, $\Delta T/\Delta t$ is the increase in temperature with time, and m is the mass concentration of MNPs [62].

From this formula, it can be seen that the heating efficiency of magnetic particles is related to the frequency of external AMF and the area enclosed by M and H curves. Theoretically, SAR will increase with the increase of magnetic field strength and frequency, as does the experimental result [63]. In addition, the properties of MNPs, including viscosity, radius, anisotropy, and collective behavior caused by surface modification, will also affect the thermal conversion efficiency [64, 65]. Table 2 lists several commercial MNP-related parameters for reference.

In MFH, coils are generally used as converters between electrical power and magnetic field energy (Fig. 3). Coils can be divided into solenoid shape [66], flat shape [67], Helmholtz's coil [68], and birdcage coil according to the shape. The first clinical MFH system, MFH® 300F, was reported in 2004 [69].

Although MFH has many advantages and application prospects, there are still many challenges in its clinical application:

(1) Real-time image guidance

A good imaging guidance can identify the location of lesions and the thermal dose of MFH, allowing doctors to predict the effect of hyperthermia [70]. It is expected to

Table 2 Basic parameters of several commercial MNPs

Particle	Manufacturer	Radius	Iron concentration	Saturation magnetization
Perimag	Micromod	130 nm	8.5 mg/mL	$H > 800$ kA/m
Synomag-50	Micromod	50 nm	10 mg/mL	$H > 800$ kA/m
Synomag-70	Micromod	70 nm	10 mg/mL	$H > 800$ kA/m
Vivotrax	Magnetic Insight	62 nm	5.5 mg/mL	/
Mag3300	Nanoeast	5–50 nm	1 mg/mL	65 emu/g Fe

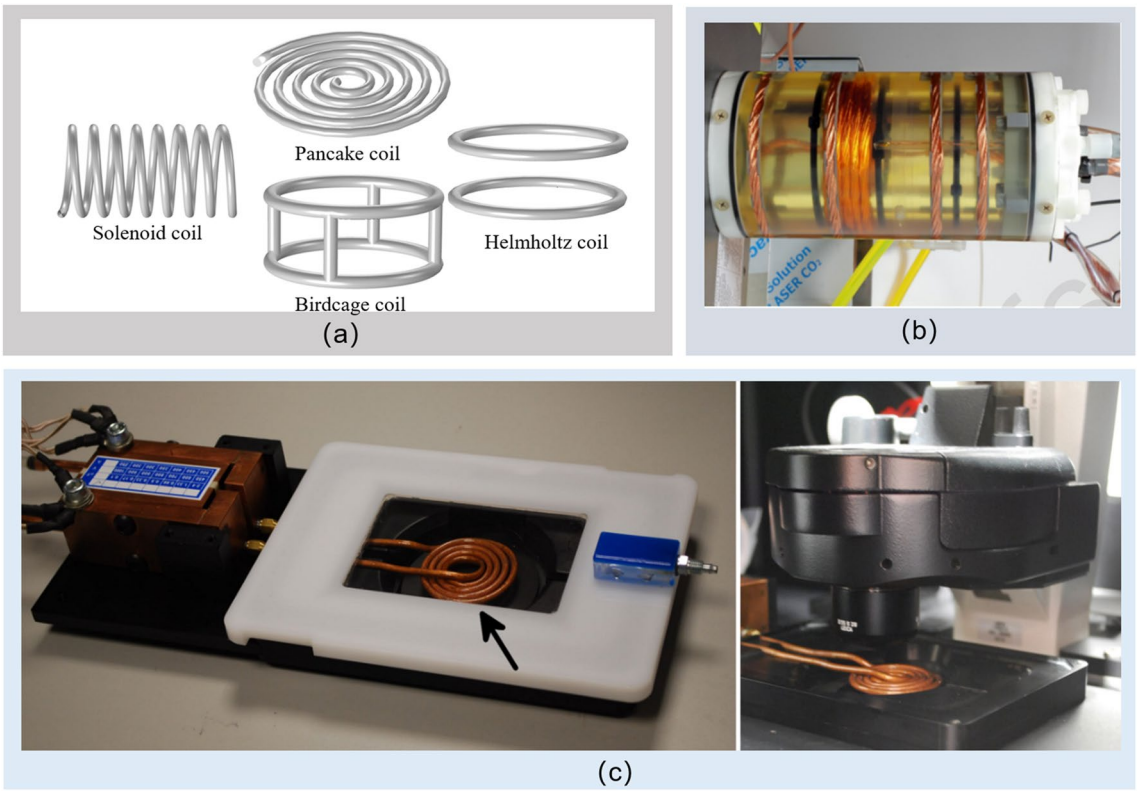

Fig. 3 MFH coils. **a** Traditional MFH coils. **b** Special thermotherapy coil in MPI. **c** Traditional MFH coil physical picture. **a** From [62]; **b** from [80]; **c** from [67]

eliminate the unnecessary risk of damaging healthy tissue and provide feedback and a basis for doctors to adjust the treatment process [71]. The aforementioned CT and MRI-guided hyperthermia cannot achieve real-time guidance, and they usually rely on pre-treatment images [72].

(2) Off-target accumulation of MNPs

After systemic administration, liver and kidneys compete with tumors for MNPs, resulting in accumulation of particles in non-targeted organs [73]. At 300 kHz, all regions of the body with MNPs are heated indiscriminately [74]. Avoiding heating off-target areas can reduce collateral thermal damage to these organs, which is important in achieving precision hyperthermia [75].

(3) Non-invasive temperature monitoring

Temperature monitoring and adjustment are important during hyperthermia [76]. It has been reported that tumor areas with hyperthermia temperatures between 41 and 45 °C are more susceptible to further damage [77]. So real-time thermal feedback can avoid temperatures that are too low or too high [78]. The existing temperature measurement technology is limited to placing a temperature sensor inside the heated tumor, which requires the sensor to be non-metallic to prevent interference with the AMF or heating during the heating process [79].

In summary, both MPI and MFH utilize the corresponding properties of MNPs for imaging and therapeutic. Now, we will compare the two methods briefly (Table 3).

Table 3 Comparison of MPI and MFH

	Purpose	Theory	Frequency of magnetic field	Amplitude of magnetic field	MNPs
MPI	Imaging	Langevin model, Debye model, etc	10–100 kHz [80]	Tens of μT to hundreds of mT [81]	Vivotrax, Perimag, etc
MFH	Therapy	Relaxation loss or hysteresis loss	100–300 kHz [50]	5–10 kA/m	Homemade EGFR-targeted MNPs [82]

Image-guided MFH

CT or MRI-Guided MFH

MFH alone cannot implement precision therapy without the help of medical image guidance. The current clinical guidance methods of MFH are mainly CT and MRI [83]. In the MFH, the density of MNP-enriched tissue regions is significantly higher than those of other normal tissue regions, which can be detected by CT [84, 85]. In clinical research, Johnnsen et al. [86] used CT imaging to develop therapeutic plans to achieve the treatment of prostate cancer. This guiding method allows for higher injection precision and thus better treatment results. MRI measures relaxation time and proton density. Clinically, contrast agents enhance the relaxation rates of water molecules around the body to obtain highly contrasting MRI images [87]. The MRI-guided MFH technology has its intrinsic advantages in providing accurate guidance and expected non-invasive temperature detection [88]. Wang et al. [89] developed a multifunctional MNP to achieve MRI-guided MFH in a breast cancer mouse model, which significantly reduced the tumor volume and the number of M2-TAMs promoted in the tumor. Corresponding materials (Fe_3O_4@ polyvinyl pyrrolidone nanotubes) for MRI-guided MFH have also been developed [90].

Compared with CT, MRI and MPI have no radiation. MRI currently uses MNPs as negative contrast agents for lymph node and liver imaging. In these areas, tissues contain a large number of phagocytes, which absorb MNPs to make the image darker [91]. This process may obscure parts of the anatomy. Other sources of endogenous contrast, such as the existence of iron deposits, may interfere with the MNP signal [92]. In addition, compared to MRI, MPI directly measures the concentration of MNPs, which are quantifiable and highly sensitive [93].

In conclusion, MPI can locate tumors more accurately, which is a significant advantage for image-guided MFH. The amount of heat deposited in the organism is directly related to the amount of MNPs, and the quantifiable nature of MPI also allows MPI to indirectly quantify the thermal dose [75].

MPI-Guided MFH

Researchers have paid attention to the combination potential of MPI and MFH. MPI and MFH work separately by utilizing the responses of MNPs to an applied AMF. Both MPI and precisely localized MFH use gradient magnetic fields. In Langevin's theory, the selection field is divided into a magnetic FFR and saturation region. Particles in the saturation region will constrain the deflection of the dipole, thus completing the confinement of the heating region, which is expected to achieve precise positioning of hyperthermia. Based on this, MFH is expected to eliminate interference from non-targeted organs during the heating process.

In 2016, Dhavalikar et al. theoretically demonstrated the possibility of combining MPI with a high-frequency-driven AMF [94]. Bauer et al. first demonstrated that a sample in a region of interest can be selectively heated with the help of a gradient field of MPI [95]. In 2017, the first combined MPI-MFH system was reported by Hensley et al. [57], which can realize selectively heat magnetic nanoparticle samples at a distance of 3 mm *in vitro* (Fig. 4). An MPI-MFH treatment platform was first demonstrated by Tay et al. in 2018 [75]. The experimenters performed selective heating and histological evaluations on a double-tumor mouse model to verify the localization of the lesion and tumor treatment capabilities of the platform (Fig. 5). According to Fig. 5, it can be clearly found that any region can be positioned and heated during the heat shock process; if there is no gradient during the heat shock process, then regions with particles in the body will be heated uniformly. In 2020, Wells et al. [96] first proposed an MPI-MFH platform based on a 3D Lissajous scanning trajectory with frequencies of around 25 kHz. In recent years, great progress has been made in research focusing on MPI-MFH. In order to have a better combination of MPI and MFH, researchers still face many problems which we will discuss in the following parts.

Targeting MPI and MFH Fusion in the Treatment of Tumors

MNPs are the only signal source for MPI visualization. The performance of MNPs is also one of the key factors to determine the quality of MPI images. In order to obtain good quality images, MNPs should have the properties of a strong response signal and slow attenuation of the signal harmonic spectrum. When MNPs are applied for MFH, they need to have a good thermal effect and temperature sensitivity. MNPs usually have magnetic core coated with a biocompatible polymer coating such as carboxyl dextran or polyethylene glycol (PEG). These outer coats have a number of functional groups that can bind to functional molecules, such as drugs or ligands. This can improve the targeting of MNPs and increase their accumulation or penetration depth in the lesion area [97, 98].

Targeted Modified MNPs

Although studies on MNPs for imaging and hyperthermia have been demonstrated, a major obstacle limiting their

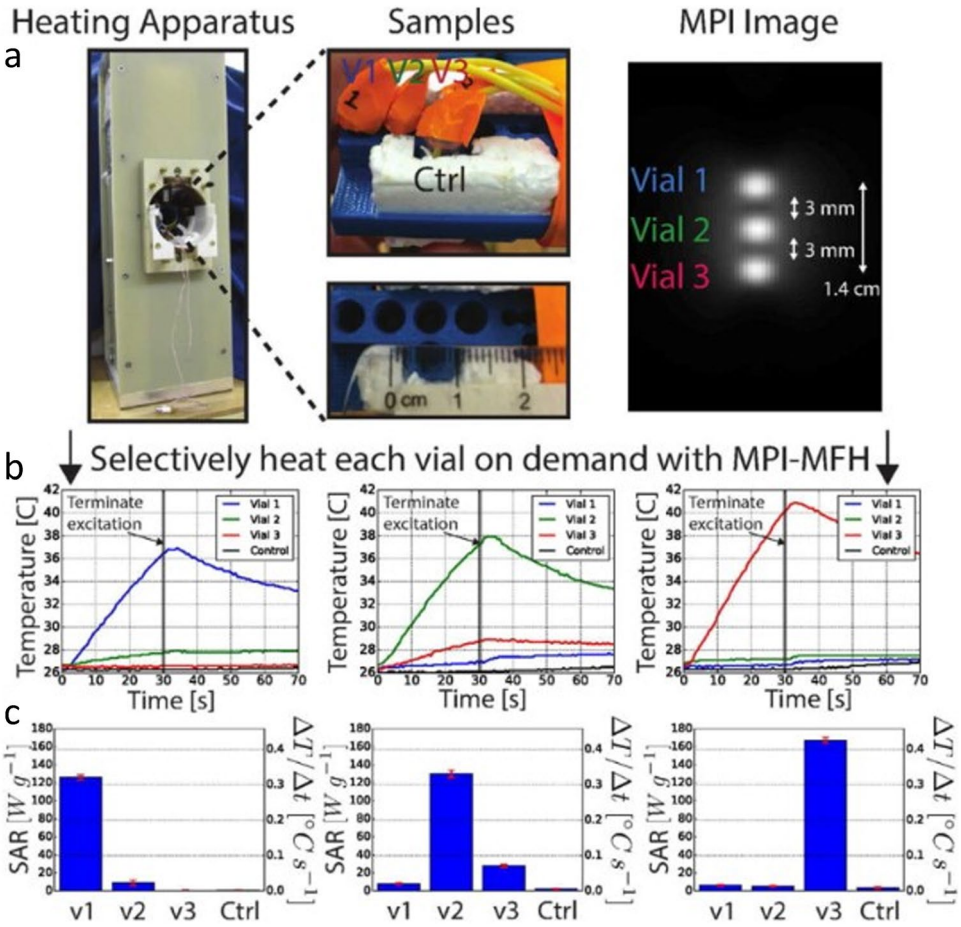

Fig. 4 *In vitro* selective heating achieved by MPI-MFH. Figure 4 is from [57]

clinical application is the insufficient concentration of particles reaching the target area after intravenous injection, resulting in an inability to accurately image and hyperthermia [99]. It has been confirmed by a large number of researches that the radius, anisotropy, structure, doping, and surface modification of particles will have a significant influence on the imaging [100] and high-temperature results [64]. There are two main ways to obtain functionalized MNPs. One way is taking advantage of the special physiological and anatomical characteristics of tumor tissues to allow for natural differences in drug distribution in the body [101]. The other is to increase uptake of magnetic particles by cells by changing the shape or aggregation state of magnetic particles or to enhance passive targeting through EPR effects, thus accumulating in tumor tissues [102]. Surface modification of targeted molecules can confer targeting properties to MNPs to significantly affect their diagnostic and therapeutic properties [103]. Current targeting molecules include antibodies [104], peptides [105], small organic molecules [106], and other biological targeting molecules [107]. Current studies have confirmed that many tumors have specific targets, such as human epidermal growth factor receptor 2 (HER-2) and luteinizing hormone-releasing hormone (LHRH) for breast cancer [108, 109], folate receptor for ovarian and cervical cancer [110], and vascular endothelial growth factor (VEGF) for glioma [111].

In MPI, the concentration of particles can be increased by targeted modification of particles, resulting in higher MPI signal intensity and better image resolution at the lesion. Tomitaka et al. combined lactoferrin with MNPs, and the resulting particles were targeted to gliomas [112]. Zhang et al. took advantage of the properties of the plectin-1 peptide targeted to pancreatic ductal adenocarcinoma and combined plectin-1 peptide and IRDye800CW with MNPs to generate pancreatic ductal adenocarcinoma-targeted probes. Uniform distribution and *in vivo* residence time were all improved [113]. Wang et al. selected the breast cancer-targeted peptide CREKA to couple with MNPs, and a stronger MPI signal than the untargeted tissue could be obtained by using this particle [114].

In MFH, the targeted modification of MNPs has a similar function with MPI, which can improve the efficiency of

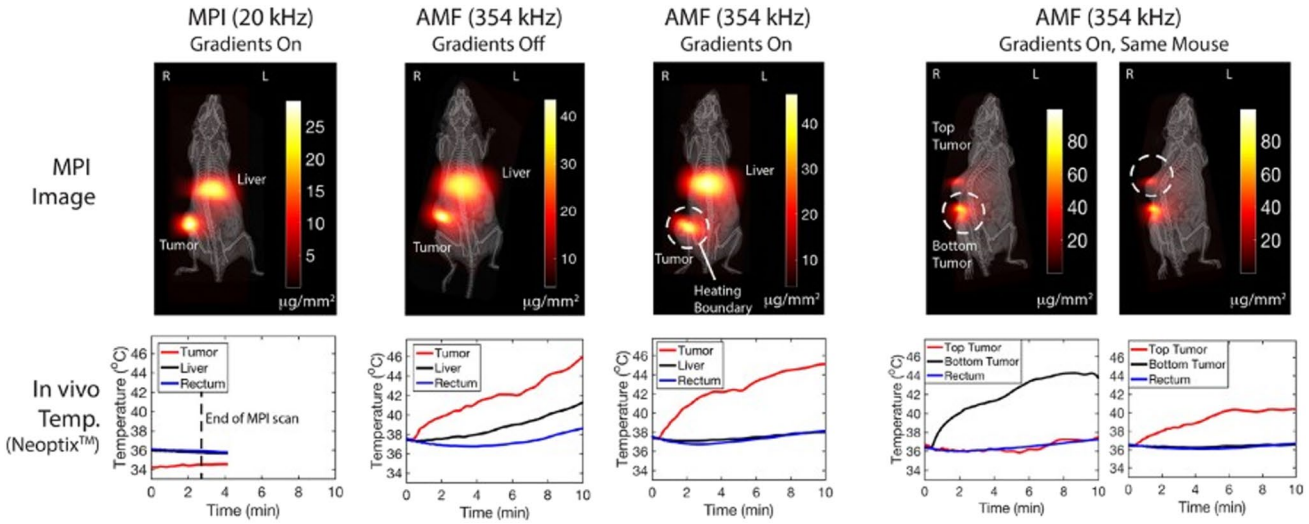

Fig. 5 *In vivo* selective heating of mice achieved by MPI-MFH. Figure 5 is from [75]

hyperthermia. We did a table (Table 4) summarizing the use of active tumor targeting in hyperthermia.

Applications of MPI-MFH Hyperthermia in the Treatment of Tumors

The application of MPI-MFH in tumors is relatively few because MPI itself is a new technology, and the combination of the two devices needs further research. Among them, the study of Du et al. [126] has opened a new horizon for us. Du et al. developed CREKA-modified MNPs using the theoretical basis that the pentapeptide CREKA can selectively bind to proteins overexpressed in certain breast cancer cells and stromal cells (Fig. 6). Such particles can target tumors and improve the uniformity of particle delivery within the tumor to obtain good MRI and MPI signals. The targeted modified particles can be uniformly distributed in the tumor and reach to ~ 43 °C

Table 4 Application of active targeting modified particles in hyperthermia

Tumor	Targeting agents	Receptors	Conditions	Refs
Hepatocellular	D-galactosamine	Asialoglycoprotein	780 kHz; 19 kA/m; 20 min	Liao et al. [115]
Cervical	PEG-FA	Folate	750 kHz; 10 Oe; 10 min	Sadhasivam et al. [116]
Adenocarcinoma	Anti-HER2 aptamer with 5′ thiol group	HER2	280 kHz; 300 A; 30 min	Pala et al. [117]
Lung	CREKA	Fibrinogen complexes	292 kHz; 58 kA/m; 30 min	Kruse et al. [118]
Prostate	Single-chain Fv antibody	γ-Seminoprotein	63 kHz; 7 kA/m; 4 min	Cui et al. [119]
Breast	^{111}In-chimeric L6 monoclonal antibody	Membrane glycoprotein	153 kHz; 1300 Oe, 1000 Oe, and 700 Oe	DeNardo et al. [120]
Breast	Anti-HER2	HER2	400 kHz; 0.8 kA/m; 5 min, 10 min	Zuvin et al. [121]
Renal cell	The Fab' fragment of the G250 antibody	MN antigen	118 kHz; 384 Oe; 30 min	Shinkai et al. [122]
Ovarian	LHRH peptide	LHRH receptors	393 kHz; 33.5 kA/m	Taratula et al. [123]
Melanoma	N-propionyl-cysteaminyl-phenol	Tyrosine analogs	118 kHz; 30.6 kA/m	Sato et al. [124]
Oral epidermoid and cervical	Folic acid	Folate receptor	Not applicable	Fan et al. [125]

quickly. In a mouse breast tumor model, the mice injected with the particles nearly disappeared after hyperthermia and did not return. This particle has great potential for precise imaging and efficient MFH.

Song et al. [127] started from MNPs and selected carbon-coated FeCo (FeCo@C-PEG) nanoparticles as the MPI tracer. When applied in a mouse model of breast cancer, it was found that FeCo@C-PEG was enriched in tumors by 4.76 times that of VivoTrax, and tumor cells also ingested significantly more FeCo@C-PEG than VivoTrax. In *in vivo* experiments, the temperature of tumors directly injected with FeCo@C-PEG can rise to 47 °C within 10 min, and the volume of tumors after 14 days was significantly smaller than that of the control group. This particle can improve image quality and conversion efficiency which can make MPI-guided MFH more effective.

Tay et al. [75] demonstrated a theranostic platform combining MPI and MFH. Using the self-developed MNPs, they first realized directional heating in the phantom. Then, MPI was used to guide MFH in glioma mouse models, and the gradient of MPI was used to achieve precise hyperthermia.

Challenges

Development of Hardware Equipment

After more than 20 years of development, MPI has come a long way in both theory and equipment. But at present, MPI hardware equipment still faces some problems, such as the need to develop a human-sized device [80], the balance between imaging performance and power consumption [128], and the need to combine with other imaging modalities to provide sufficient information [129].

Real-time simultaneous imaging and hyperthermia is possible, because MNPs can generate MPI signals during heating. Usually, the operating frequencies of the two are significantly different. The operating frequency of MPI is roughly 10 kHz ~ 100 kHz [130], and the operating frequency of MFH is roughly 100 kHz ~ 300 kHz [50]. There are two options for combining the two. First, the fixed operating frequency is between 20 and 40 kHz, which theoretically can achieve simultaneous imaging and

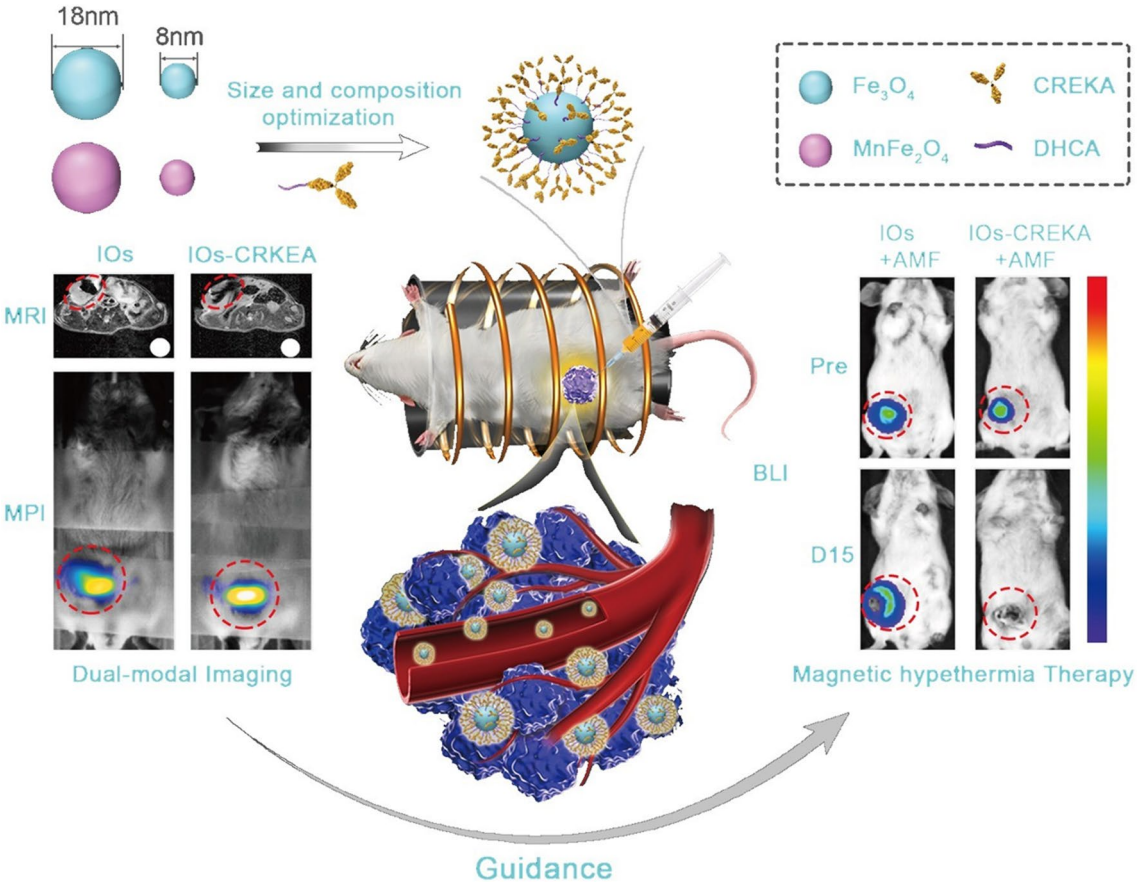

Fig. 6 CREKA-modified MNPs for bi-modal MRI/MPI-guided magnetothermal therapy. Figure 6 is from [126]

hyperthermia. However, we need to give MNPs multi-dimensional excitation to achieve the same thermal effect as in high frequency [96]. We believe a better way is to work at a low frequency and high frequency in time-sharing, but the complexity of the equipment could be significantly increased.

MNP Optimization

The response of MNPs to AMF can achieve both imaging and MFH. Translating this potential into clinical applications requires the development of MNPs. Therefore, it is urgent to prepare MNPs that have excellent imaging capabilities, thermal efficiency, temperature monitoring capabilities, and biocompatibility.

SAR and PNS Limits

The AMF can affect the human body through peripheral nerve stimulation (PNS) or induction eddy current heating *in vivo*, and these magnetic field changes have potential risks for the human body [53]. For frequencies below 100 kHz, it should be particularly concerned by electrical stimulation risks; while for higher frequencies, the primary considerations should be thermal heating [131]. During the MPI-guided MFH process, we must consider the two limits of PNS and SAR. For the application of the thoracic body, the limit of PNS is about 3 mT μ_0^{-1} [132], and the limit of PNS is linearly related to the magnetic directional cross-section of the body, so it is safe to apply 6 mT μ_0^{-1} [53] to the head and 10 mTμ_0^{-1} to the whole body. For the SAR, the spatial average SAR exposed to tissues in public and controlled environments is 2 W/kg and 10 W/kg [133]. Currently, no more specific data on MPI-guided MFH PNS and SAR advice values is available. The limiting of PNS is necessary to prevent excessive muscle and nerve stimulation, and the limiting of SAR is crucial to prevent system temperature rise [130]. However, the importance of these two limits for MPI-guided MFH is undeniable.

Prospect of Application

A significant advantage of MPI is that the signal can be quantified. On the combined MPI and MFH platform, this advantage can be translated into the evaluation of therapeutic effects. In Ohki et al.'s study, regions of interest were mapped using MPI, which was used to quantitatively compare the effects of tumor hyperthermia alone and hyperthermia combined with radiotherapy [134]. Numerous studies have shown that the combination of radiotherapy or chemotherapy with hyperthermia is more helpful in the treatment of cancer [83]. Other studies have shown that hyperthermia can be combined with gene therapy or immunotherapy [135]. Pan et al. demonstrated that combined MFH and immunotherapy have great potential in primary and metastatic tumors [136]. MPI-MFH is expected to enable quantitative assessment of the efficacy of hyperthermia alone and in combination therapy. In addition, MPI-MFH also has great potential for controlled release and targeted delivery of drugs and can be used in other non-cancer diseases.

Conclusion

MPI-MFH is expected to realize the combination of diagnosis and treatment, allowing MPI images to accurately locate the lesion and predict the magnetic thermal effect at the same time, which helps doctors to plan and adjust the magnetic thermal plan. Currently, MPI-MFH has achieved millimeter-precise guided heating which has been demonstrated in mice. However, MPI-MFH still has a long way to go. The development of MPI-MFH devices, the design of MNPs that consider both MPI and MFH performance, and the successful clinical applications in humans are all urgent problems that need to be solved. It is encouraging that more and more scholars are noticing the potential of MPI-MFH and are proposing creative solutions to these problems. We believe that in the future, MPI-MFH, combined with other therapies and technologies, will provide better options to treat cancer and even non-cancer diseases.

Funding This work was supported in part by the National Key Research and Development Program of China under Grant: 2017YFA0700401; the National Nature Science Foundation of China under Grants: 62027901, 81827808, 81930053, and 81227901; the Beijing Natural Science Foundation (JQ22023); the CAS Youth Innovation Promotion Association under Grant: Y2022055; the Guangdong Key Research and Development Program of China (2021B0101420005); and the Project of High-Level Talents Team Introduction in Zhuhai City (Zhuhai HLHPTP201703).

Declarations

Conflict of Interest The authors declare no competing interests.

References

1. Chen X, Wong STC (2014) Cancer theranostics: an introduction. In: Chen X, Wong STC (eds) Cancer Theranostics. Academic, pp 3–4
2. Lee YT, Tan YJ, Oon CE (2018) Molecular targeted therapy: treating cancer with specificity. Eur J Pharmacol 834:188–196
3. Matsen CB, Neumayer LA (2013) Breast cancer: a review for the general surgeon. JAMA Surg 148:971–979
4. Blumenschein GR, Distefano A, Caderao J et al (1997) Multimodality therapy for locally advanced and limited stage IV breast

cancer: the impact of effective non-cross-resistant late-consolidation chemotherapy. Clin Cancer Res 3:2633–2637
5. Park W, Chawla A, O'Reilly EM (2021) Pancreatic cancer: a review. JAMA - J Am Med Assoc 326:851–862
6. Hughes JR, Parsons JL (2020) Flash radiotherapy: current knowledge and future insights using proton-beam therapy. Int J Mol Sci 21:1–14
7. Baskar R, Lee KA, Yeo R, Yeoh KW (2012) Cancer and radiation therapy: current advances and future directions. Int J Med Sci 9:193–199
8. Mohan R, Bortfeld T (2011) Proton therapy: clinical gains through current and future treatment programs. Front Radiat Ther Oncol 43:440–464
9. Dinesh Mayani D (2011) Proton therapy for cancer treatment. J Oncol Pharm Pract 17:186–190
10. Mohan R, Grosshans D (2017) Proton therapy – present and future. Adv Drug Deliv Rev 109:26–44. https://doi.org/10.1016/j.addr.2016.11.006
11. Nygren P (2001) What is cancer chemotherapy? Acta Oncol (Madr) 40:166–174
12. Chari RVJ (2008) Targeted cancer therapy: conferring specificity to cytotoxic drugs. Acc Chem Res 41:98–107
13. Galluzzi L, Humeau J, Buqué A et al (2020) Immunostimulation with chemotherapy in the era of immune checkpoint inhibitors. Nat Rev Clin Oncol 17:725–741
14. Farzin L, Saber R, Sadjadi S et al (2022) Nanomaterials-based hyperthermia: a literature review from concept to applications in chemistry and biomedicine. J Therm Biol 104:103201
15. Harmon BV, Takano YS, Winterford CM, Gobe GC (1991) The role of apoptosis in the response of cells and tumours to mild hyperthermia. Int J Radiat Biol 59:489–501
16. van Oorschot B, Granata G, Di Franco S et al (2016) Targeting DNA double strand break repair with hyperthermia and DNA-PKcs inhibition to enhance the effect of radiation treatment. Oncotarget 7:65504–65513
17. Schildkopf P, Ott OJ, Frey B et al (2010) Biological rationales and clinical applications of temperature controlled hyperthermia - implications for multimodal cancer treatments. Curr Med Chem 17:3045–3057
18. Lee S, Son B, Park G et al (2018) Immunogenic effect of hyperthermia on enhancing radiotherapeutic efficacy. Int J Mol Sci 19:2795
19. Schneider CS, Woodworth GF, Vujaskovic Z, Mishra MV (2020) Radiosensitization of high-grade gliomas through induced hyperthermia: review of clinical experience and the potential role of MR-guided focused ultrasound. Radiother Oncol 142:43–51
20. Roussakow S (2017) Neo-adjuvant chemotherapy alone or with regional hyperthermia for soft-tissue sarcoma. Lancet Oncol 18:e629
21. Deger S, Böhmer D, Rüter A et al (2003) Interstitial hyperthermia using self-regulating thermoseeds combined with conformal radiation therapy. Eur Urol Suppl 2:136
22. Brero F, Calzolari P, Albino M et al (2023) Proton therapy, magnetic nanoparticles and hyperthermia as combined treatment for pancreatic BxPC3 tumor cells. Nanomaterials 13:1–17
23. Singh A, Jain S, Sahoo SK (2020) Magnetic nanoparticles for amalgamation of magnetic hyperthermia and chemotherapy: an approach towards enhanced attenuation of tumor. Mater Sci Eng C 110:110695
24. Nagata Y, Hiraoka M, Nishimura Y et al (1997) Clinical results of radiofrequency hyperthermia for malignant liver tumors. Int J Radiat Oncol Biol Phys 38:359–365
25. van Valenberg H, Colombo R, Witjes F (2016) Intravesical radiofrequency-induced hyperthermia combined with chemotherapy for non-muscle-invasive bladder cancer. Int J Hyperth 32:351–362
26. Hildebrandt B, Wust P, Gellermann J et al (2004) Treatment of locally recurrent rectal cancer with special focus on regional pelvic hyperthermia. Onkologie 27:506–511
27. Franco JVA, Garegnani L, Liquitay CME et al (2022) Transurethral microwave thermotherapy for benign prostatic hyperplasia: an updated Cochrane review. World J Mens Health 40:127–138
28. Moradpoor R, Aledavood SA, Rajabi O et al (2017) Enhancement of cisplatin efficacy by gold nanoparticles or microwave hyperthermia? An in vitro study on a melanoma cell line. Int J Cancer Manag 10:1–8
29. Wu F (2014) High intensity focused ultrasound: a noninvasive therapy for locally advanced pancreatic cancer. WORLD J Gastroenterol 20:16480–16488
30. Kim Y-S (2017) Clinical application of high-intensity focused ultrasound ablation for uterine fibroids. Biomed Eng Lett 7:99–105
31. Lang BH, Wu ALH (2018) The efficacy and safety of high-intensity focused ultrasound ablation of benign thyroid nodules. Ultrasonography 37:89–97
32. Zhou Z, Yan Y, Hu K et al (2017) Autophagy inhibition enabled efficient photothermal therapy at a mild temperature. Biomaterials 141:116–124
33. Monitoring RT, Ptt IG (2007) Accurate and real-time temperature monitoring during MR imaging guided PTT. Nano Lett 20:2522–2529
34. Yu Y, Tang D, Liu C et al (2022) Biodegradable polymer with effective near-infrared-II absorption as a photothermal agent for deep tumor therapy. Adv Mater 34:2105976
35. Deng K, Li C, Huang S et al (2017) Recent progress in near infrared light triggered photodynamic therapy. Small 13:170229
36. Yue C, Zhang C, Alfranca G et al (2016) Near-infrared light triggered ros-activated theranostic platform based on ce6-cpt-ucnps for simultaneous fluorescence imaging and chemo-photodynamic combined therapy. Theranostics 6:456–469
37. Buchholz TA, Ali S, Hunt KK (2020) Hyperthermia plus re-irradiation in the management of unresectable locoregional recurrence of breast cancer in Previously irradiated sites reply. J Clin Oncol 38:3576–3577
38. Lei Z, Wang Y, Wang J et al (2020) Evaluation of cytoreductive surgery with or without hyperthermic intraperitoneal chemotherapy for stage III epithelial ovarian cancer. JAMA Netw open 3:e2013940
39. Yu MK, Kim D, Lee IH et al (2011) Image-guided prostate cancer therapy using aptamer-functionalized thermally cross-linked superparamagnetic iron oxide nanoparticles. Small 7:2241–2249
40. Xu H, Zong H, Ma C et al (2017) Evaluation of nano-magnetic fluid on malignant glioma cells. Oncol Lett 13:677–680
41. Gleich B, Weizenecker J (2005) Tomographic imaging using the nonlinear response of magnetic particles. Nature 435:1214–1217
42. Sedlacik J, Frölich A, Spallek J et al (2016) Magnetic particle imaging for high temporal resolution assessment of aneurysm hemodynamics. PLoS One 11:1–12
43. Weizenecker J, Gleich B, Rahmer J et al (2009) Three-dimensional real-time in vivo magnetic particle imaging. Phys Med Biol 54:L1–L10
44. Them K, Salamon J, Szwargulski P et al (2016) Increasing the sensitivity for stem cell monitoring in system-function based magnetic particle imaging. Phys Med Biol 61:3279–3290
45. Zheng B, Von See MP, Yu E et al (2016) Quantitative magnetic particle imaging monitors the transplantation, biodistribution, and clearance of stem cells in vivo. Theranostics 6:291–301
46. Yu EY, Bishop M, Zheng B et al (2017) Magnetic particle imaging: a novel in vivo imaging platform for cancer detection. NANO Lett 17:1648–1654
47. Ludewig P, Gdaniec N, Sedlacik J et al (2017) Magnetic particle imaging for real-time perfusion imaging in acute stroke. ACS Nano 11:10480–10488

48. Knopp T, Gdaniec N, Möddel M (2017) Magnetic particle imaging: from proof of principle to preclinical applications. Phys Med Biol 62:R124–R178
49. Pablico-Lansigan MH, Situ SF, Samia ACS (2013) Magnetic particle imaging: advancements and perspectives for real-time in vivo monitoring and image-guided therapy. Nanoscale 5:4040–4055
50. Healy S, Bakuzis AF, Goodwill PW et al (2022) Clinical magnetic hyperthermia requires integrated magnetic particle imaging. Wiley Interdiscip Rev Nanomed Nanobiotechnol 14:e1779
51. Ludewig P, Graeser M, Forkert ND et al (2022) Magnetic particle imaging for assessment of cerebral perfusion and ischemia. Wiley Interdiscip Rev Nanomedicine Nanobiotechnology 14:e1757
52. Vogel P, Ruckert MA, Klauer P et al (2014) Traveling wave magnetic particle imaging. IEEE Trans Magn 33:400–407
53. Graeser M, Thieben F, Szwargulski P et al (2019) Human-sized magnetic particle imaging for brain applications. Nat Commun 10:1–17
54. Mattingly E, Mason EE, Śliwiak M, Wald LL (2022) Drive and receive coil design for a human-scale MPI system. Int J Magn Part Imaging 8:8–11
55. Chandrasekharan P, Tay ZW, Zhou XY et al (2018) A perspective on a rapid and radiation-free tracer imaging modality, magnetic particle imaging, with promise for clinical translation. Br J Radiol 91:20180326
56. Salamon J, Dieckhoff J, Kaul MG et al (2020) Visualization of spatial and temporal temperature distributions with magnetic particle imaging for liver tumor ablation therapy. Sci Rep 10:7480
57. Hensley D, Tay ZW, Dhavalikar R et al (2017) Combining magnetic particle imaging and magnetic fluid hyperthermia in a theranostic platform. Phys Med Biol 62:3483–3500
58. Zhong J, Schilling M, Ludwig F (2021) Simultaneous imaging of magnetic nanoparticle concentration, temperature, and viscosity. Phys Rev Appl 16:054005
59. Utkur M, Saritas EU (2022) Simultaneous temperature and viscosity estimation capability via magnetic nanoparticle relaxation. Med Phys 49:2590–2601
60. Chang M, Hou Z, Wang M et al (2021) Recent advances in hyperthermia therapy-based synergistic immunotherapy. Adv Mater 33:2004788
61. Rosensweig RE (2002) Heating magnetic fluid with alternating magnetic field. J Magn Magn Mater 252:370–374
62. Cabrera D, Rubia-Rodríguez I, Garaio E et al (2018) Instrumentation for magnetic hyperthermia. In: Fratila RM, Fuente JMDL (eds) Nanomaterials for Magnetic and Optical Hyperthermia Applications, 1st edn. Elsevier, pp 111–120
63. Dennis CL, Jackson AJ, Borchers JA et al (2009) Nearly complete regression of tumors via collective behavior of magnetic nanoparticles in hyperthermia. Nanotechnology 20:395103
64. Deatsch AE, Evans BA (2014) Heating efficiency in magnetic nanoparticle hyperthermia. J Magn Magn Mater 354:163–172
65. Sohail A, Ahmad Z, Beg OA et al (2017) A review on hyperthermia via nanoparticle-mediated therapy. Bull Cancer 104:452–461
66. Zhao Q, Wang L, Cheng R et al (2012) Magnetic nanoparticle-based hyperthermia for head & neck cancer in mouse models. Theranostics 2:113–121
67. Blanco-Andujar C, Ortega D, Southern P et al (2016) Real-time tracking of delayed-onset cellular apoptosis induced by intracellular magnetic hyperthermia. Nanomedicine 11:121–136
68. Nieskoski MD, Trembly BS (2014) Comparison of a single optimized coil and a Helmholtz pair for magnetic nanoparticle hyperthermia. IEEE Trans Biomed Eng 61:1642–1650
69. Gneveckow U, Jordan A, Scholz R et al (2004) Description and characterization of the novel hyperthermia- and thermoablation-system MFH (R) 300F for clinical magnetic fluid hyperthermia. Med Phys 31:1444–1451
70. Hu S, Kang H, Baek Y et al (2018) Real-time imaging of brain tumor for image-guided surgery. Adv Healthc Mater 7:e1800066
71. Ellis S, Rieke V, Kohi M, Westphalen AC (2013) Clinical applications for magnetic resonance guided high intensity focused ultrasound (MRgHIFU): Present and future. J Med Imaging Radiat Oncol 57:391–399
72. Fernando R, Downs J, Maples D, Ranjan A (2013) MRI-guided monitoring of thermal dose and targeted drug delivery for cancer therapy. Pharm Res 30:2709–2717
73. Wilhelm S, Tavares AJ, Dai Q et al (2016) Analysis of nanoparticle delivery to tumours. Nat Rev Mater 1:16014
74. Lu Y, Rivera-Rodriguez A, Tay ZW et al (2020) Combining magnetic particle imaging and magnetic fluid hyperthermia for localized and image-guided treatment. Int J Hyperth 37:141–154
75. Tay ZW, Chandrasekharan P, Chiu-Lam A et al (2018) Magnetic particle imaging-guided heating in vivo using gradient fields for arbitrary localization of magnetic hyperthermia therapy. ACS Nano 12:3699–3713
76. Shaterabadi Z, Nabiyouni G, Soleymani M (2018) Physics responsible for heating efficiency and self-controlled temperature rise of magnetic nanoparticles in magnetic hyperthermia therapy. Prog Biophys Mol Biol 133:9–19
77. Chu KF, Dupuy DE (2014) Thermal ablation of tumours: biological mechanisms and advances in therapy. Nat Rev Cancer 14:199–208
78. Ximendes E, Marin R, Shen Y et al (2021) Infrared-emitting multimodal nanostructures for controlled in vivo magnetic hyperthermia. Adv Mater 33:e2100077
79. Mohri K, Uchiyama T, Shen LP et al (2002) Amorphous wire and CMOS IC-based sensitive micromagnetic sensors utilizing magnetoimpedance (MI) and stress-impedance (SI) effects. IEEE Trans Magn 38:3063–3068
80. Neumann A, Gräfe K, von Gladiss A et al (2022) Recent developments in magnetic particle imaging. J Magn Magn Mater 550:169037
81. Goodwill PW, Conolly SM (2010) The X-space formulation of the magnetic particle imaging process: 1-D signal, resolution, bandwidth, SNR, SAR, and magnetostimulation. IEEE Trans Med Imaging 29:1851–1859
82. Sadhukha T, Wiedmann TS, Panyam J (2013) Inhalable magnetic nanoparticles for targeted hyperthermia in lung cancer therapy. Biomaterials 34:5163–5171
83. Maier-Hauff K, Ulrich F, Nestler D et al (2011) Efficacy and safety of intratumoral thermotherapy using magnetic iron-oxide nanoparticles combined with external beam radiotherapy on patients with recurrent glioblastoma multiforme. J Neurooncol 103:317–324
84. Attaluri A, Ma R, Zhu L (2011) Using microCT imaging Tetchnique to quantify heat generation distribution induced by magnetic nanoparticles for cancer treatments. J Heat Transfer 133:15–17
85. Lebrun A, Manuchehrabadi N, Attaluri A et al (2013) Microct image-generated tumour geometry and sar distribution for tumour temperature elevation simulations in magnetic nanoparticle hyperthermia. Int J Hyperth 29:730–738
86. Johannsen M, Gneveckow U, Eckelt L et al (2005) Clinical hyperthermia of prostate cancer using magnetic nanoparticles: presentation of a new interstitial technique. Int J Hyperth 21:637–647
87. Mornet S, Vasseur S, Grasset F, Duguet E (2004) Magnetic nanoparticle design for medical diagnosis and therapy. J Mater Chem 14:2161–2175
88. Cantillon-Murphy P, Wald LL, Zahn M, Adalsteinsson E (2010) Proposing magnetic nanoparticle hyperthermia in low-field MRI. Concepts Magn Reson Part A Bridg Educ Res 36:36–47
89. Wang W, Li F, Li S et al (2021) M2 macrophage-targeted iron oxide nanoparticles for magnetic resonance image-guided magnetic hyperthermia therapy. J Mater Sci Technol 81:77–87

90. Wang X, Pan F, Xiang Z et al (2020) Magnetic Fe_3O_4@PVP nanotubes with high heating efficiency for MRI-guided magnetic hyperthermia applications. Mater Lett 262:127187
91. Fortuin AS, Brüggemann R, van der Linden J et al (2018) Ultra-small superparamagnetic iron oxides for metastatic lymph node detection: back on the block. Wiley Interdiscip Rev Nanomedicine Nanobiotechnology 10:1–10
92. Bulte JWM (2019) Superparamagnetic iron oxides as MPI tracers: a primer and review of early applications. Adv Drug Deliv Rev 138:293–301
93. Paysen H, Loewa N, Stach A et al (2020) Cellular uptake of magnetic nanoparticles imaged and quantified by magnetic particle imaging. Sci Rep 10:1–8
94. Dhavalikar R, Rinaldi C (2016) Theoretical predictions for spatially-focused heating of magnetic nanoparticles guided by magnetic particle imaging field gradients. J Magn Magn Mater 419:267–273
95. Bauer LM, Situ SF, Griswold MA, Samia ACS (2016) High-performance iron oxide nanoparticles for magnetic particle imaging-guided hyperthermia (hMPI). Nanoscale 8:12162–12169
96. Wells J, Twamley S, Sekar A et al (2020) Lissajous scanning magnetic particle imaging as a multifunctional platform for magnetic hyperthermia therapy. Nanoscale 12:18342–18355
97. Kratz H, Taupitz M, De Schellenberger AA et al (2018) Novel magnetic multicore nanoparticles designed for MPI and other biomedical applications: from synthesis to first in vivo studies. PLoS One 13:1–22
98. Chen L, Wu Y, Wu H et al (2019) Magnetic targeting combined with active targeting of dual-ligand iron oxide nanoprobes to promote the penetration depth in tumors for effective magnetic resonance imaging and hyperthermia. Acta Biomater 96:491–504
99. Giouroudi I, Kosel J (2010) Recent progress in biomedical applications of magnetic nanoparticles. Recent Pat Nanotechnol 4:111–118
100. Lu C, Han LB, Wang JN et al (2021) Engineering of magnetic nanoparticles as magnetic particle imaging tracers. Chem Soc Rev 50:8102–8146
101. Hilger I (2013) In vivo applications of magnetic nanoparticle hyperthermia. Int J Hyperth 29:828–834
102. Fourmy D, Carrey J, Gigoux V (2015) Targeted nanoscale magnetic hyperthermia: challenges and potentials of peptide-based targeting. Nanomedicine 10:893–896
103. Liu X, Zhang H, Zhang T et al (2022) Progress in biomedical engineering magnetic nanomaterials-mediated cancer diagnosis and therapy progress in biomedical engineering. Prog Biomed Eng 4:012005
104. Tang L, Casas J, Venkataramasubramani M (2013) Magnetic nanoparticle mediated enhancement of localized surface plasmon resonance for ultrasensitive bioanalytical assay in human blood plasma. Anal Chem 85:1431–1439
105. Wadajkar AS, Menon JU, Tsai YS et al (2013) Prostate cancer-specific thermo-responsive polymer-coated iron oxide nanoparticles. Biomaterials 34:3618–3625
106. Veiseh O, Gunn JW, Zhang M (2010) Design and fabrication of magnetic nanoparticles for targeted drug delivery and imaging. Adv Drug Deliv Rev 62:284–304
107. Yang M, Cheng K, Qi S et al (2013) Affibody modified and radiolabeled gold-iron oxide hetero-nanostructures for tumor PET, optical and MR imaging. Biomaterials 34:2796–2806
108. Chen JS, Chen J, Bhattacharjee S et al (2020) Functionalized nanoparticles with targeted antibody to enhance imaging of breast cancer *in vivo*. J Nanobiotechnology 18:135
109. Nian D, Shi P, Sun J et al (2019) Application of luteinizing hormone-releasing hormone–ferrosoferric oxide nanoparticles in targeted imaging of breast tumors. J Int Med Res 47:1749–1757
110. Luong D, Sau S, Kesharwani P, Iyer AK (2017) Polyvalent folate-dendrimer-coated iron oxide theranostic nanoparticles for simultaneous magnetic resonance imaging and precise cancer cell targeting. Biomacromol 18:1197–1209
111. Abakumov M, Nukolova NV, Sokolsky-Papkov M et al (2015) VEGF-targeted magnetic nanoparticles for MRI visualization of brain tumor. Nanomedicine 11:825–833
112. Tomitaka A, Arami H, Gandhi S, Krishnan KM (2015) Lactoferrin conjugated iron oxide nanoparticles for targeting brain glioma cells in magnetic particle imaging. Nanoscale 7:16890–16898
113. Zhang W, Liang X, Zhu L et al (2022) Optical magnetic multimodality imaging of plectin-1-targeted imaging agent for the precise detection of orthotopic pancreatic ductal adenocarcinoma in mice. EBioMedicine 80:104040
114. Wang G, Li W, Shi G et al (2022) Sensitive and specific detection of breast cancer lymph node metastasis through dual-modality magnetic particle imaging and fluorescence molecular imaging: a preclinical evaluation. Eur J Nucl Med Mol Imaging 49:2723–2734
115. Liao SH, Liu CH, Bastakoti BP, Suzuki N, Chang Y, Yamauchi Y, Lin FH, Wu KC (2015) Functionalized magnetic iron oxide/alginate core-shell nanoparticles for targeting hyperthermia. Int J Nanomedicine 10:3315–3327
116. Sadhasivam S, Savitha S, Wu CJ et al (2015) Carbon encapsulated iron oxide nanoparticles surface engineered with polyethylene glycol-folic acid to induce selective hyperthermia in folate over expressed cancer cells. Int J Pharm 480:8–14
117. Pala K, Serwotka A, Jeleń F et al (2013) Tumor-specifc hyperthermia with aptamer-tagged superparamagnetic nanoparticles. Int J Nanomed 9:67–76
118. Kruse AM, Meenach SA, Anderson KW, Hilt JZ (2014) Synthesis and characterization of CREKA-conjugated iron oxide nanoparticles for hyperthermia applications. Acta Biomater 10:2622–2629
119. Cui D, Han Y, Li Z et al (2009) Fluorescent magnetic nanoprobes for in vivo targeted imaging and hyperthermia therapy of prostate Cancer. Nano Biomed Eng 1:61–74
120. DeNardo SJ, DeNardo GL, Miers LA et al (2005) Development of tumor targeting bioprobes (111In-chimeric L6 monoclonal antibody nanoparticles) for alternating magnetic field cancer therapy. Clin Cancer Res 11:7087–7093
121. Zuvin M, Kocak M, Unal O et al (2019) Nanoparticle based induction heating at low magnitudes of magnetic field strengths for breast cancer therapy. J Magn Magn Mater 483:169–177
122. Shinkai M, Le B, Honda H et al (2001) Targeting hyperthermia for renal cell carcinoma using human MN antigen-specific magnetoliposomes. Japanese J Cancer Res 92:1138–1146
123. Taratula O, Dani RK, Schumann C et al (2013) Multifunctional nanomedicine platform for concurrent delivery of chemotherapeutic drugs and mild hyperthermia to ovarian cancer cells. Int J Pharm 458:169–180
124. Sato M, Yamashita T, Ohkura M et al (2009) N-propionylcysteaminylphenol-magnetite conjugate (NPrCAP/M) Is a nanoparticle for the targeted growth suppression of melanoma cells. J Invest Dermatol 129:2233–2241
125. Fan C, Gao W, Chen Z et al (2011) Tumor selectivity of stealth multi-functionalized superparamagnetic iron oxide nanoparticles. Int J Pharm 404:180–190
126. Du Y, Liu X, Liang Q et al (2019) Optimization and design of magnetic ferrite nanoparticles with uniform tumor distribution for highly sensitive MRI/MPI performance and improved magnetic hyperthermia therapy. Nano Lett 19:3618–3626
127. Song G, Kenney M, Chen YS et al (2020) Carbon-coated FeCo nanoparticles as sensitive magnetic-particle-imaging tracers with photothermal and magnetothermal properties. Nat Biomed Eng 4:325–334. https://doi.org/10.1038/s41551-019-0506-0

128. Soydan DA, Karaca S, Top CB (2022) Increasing the efficiency of open-sided field free line scanning MPI system using silicon-steel core. Int J Magn Part Imaging 8:8–10
129. Franke J, Baxan N, Lehr H et al (2020) Hybrid MPI-MRI system for dual-modal in situ cardiovascular assessments of real-time 3D blood flow quantification - a pre-clinical in vivo feasibility investigation. IEEE Trans Med Imaging 39:4335–4345
130. Chandrasekharan P, Tay ZW, Hensley D et al (2020) Using magnetic particle imaging systems to localize and guide magnetic hyperthermia treatment: tracers, hardware, and future medical applications. Theranostics 10:2965–2981
131. International Commission on Non-Ionizing Radiation Protection (ICNIRP) (1993) Guidelines for limiting exposure to time-varying electric, magnetic, and electromagnetic fields (up to 300 GHz). International Commission on Non-Ionizing Radiation Protection. Health Phys 74:494–522
132. Schmale I, Gleich B, Schmidt J et al (2013) Human PNS and SAR study in the renquency range from 24 to 162 hHz. Int Work Magn Part Imag 259:22335
133. Bailey W, Bodemann R et al (2019) Synopsis of IEEE Std C95.1™-2019 "IEEE standard for safety levels with respect to human exposure to electric, magnetic, and electromagnetic fields, 0 Hz to 300 GHz." IEEE Access 7:171346–171356
134. Ohki A, Kuboyabu T, Aoki M et al (2016) Quantitative evaluation of tumor response to combination of magnetic hyperthermia treatment and radiation therapy using magnetic particle imaging. Int J Nanomed Nanosurg 2(3). https://doi.org/10.16966/2470-3206.117
135. Wust P, Hildebrandt B, Sreenivasa G et al (2002) Hyperthermia in combined treatment of cancer. Lancet Oncol 3:487–497
136. Pan J, Hu P, Guo Y et al (2020) Combined magnetic hyperthermia and immune therapy for primary and metastatic tumor treatments. ACS Nano 14:1033–1044